Laser Welding and Process Monitoring Applications for Advanced Manufacturing of Batteries and Fuel Cells

Rahul Patwa, H. Herfurth, S. Heinemann, H. Pantsar, and B. Regaard
Fraunhofer Center for Laser Technology

Golam Newaz and Mohammad Hailat
Institute for Manufacturing Research

Abstract

Recently, battery-based hybridization of gasoline and diesel engines has become a rapidly expanding global market. A lot of research and development activities have been focused on both advanced batteries and fuel cells to achieve their efficient mass production capabilities and drive this technology into successful commercialization.

A variety of joining processes are required for the assembly of cells and modules. This paper focuses on the laser welding applications for similar and dissimilar materials. Materials that have been investigated are Cu, Al, and stainless steel. The goal is to define the key laser processing parameters based on characterization of the joints by means of mechanical failure tests and bond area analysis. This study also includes a camera-based process monitoring technique to monitor the behavior of the keyhole and the melt pool during the welding process. An example of sealing Al cans used as battery housings illustrates the successful application of laser technology.

Introduction

Significant attention has been given worldwide to the rapid increase in energy demand and global environmental concerns. A general consensus exist that the continued reliance of automobiles on fossil fuels, which consume almost 45% of all fossil fuels produced, is one of the primary causes for the global warming.[(1)] Reducing the demand for foreign oil has been widely recognized as a faster, cleaner, and cheaper path to energy security.

One approach to tackle some of these challenges is to use the existing resources more efficiently. With regard to automobiles, battery-based hybridization of gasoline and diesel engines is happening at a fast pace, because it combines the benefits of high fuel economy and low emissions with the power, range, and convenience of traditional gasoline and diesel-powered vehicles. According to a report by The Boston Consulting Group, an estimated 14 million electric and hybrid cars may be sold in 2020 in the world's four largest automotive markets - Western Europe, North America, Japan, and China - up from some 480,000 in 2008.[(2)]

A variety of systems such as hybrid electric vehicles (HEV), plug-in hybrid electric vehicles (PHEV), and electric vehicles (EV) are either on the market or currently under development. One of the enabling factors for the development of new hybrid systems for vehicles are significant advancements in battery technology. Most developers believe that the Li-ion batteries will be leading this emerging market.[(3)] In addition to reliability and safety,[(4)] battery cost will play an important factor for a broad market acceptance of PHEVs using Li-ion technology. Battery pricing will be significantly impacted by material cost and manufacturing cost in mass production.

A variety of cutting, joining, and sealing operations are required for the production of electrodes and the assembly of cells and modules. Figure 1 shows the basic elements of a cylindrical battery cell. The electrode package consists of coated metal foils that are wound to a roll. This electrode package is hermetically sealed in a metal can and electrically connected to the outside terminals. Cells with planar shape and stacked electrodes cells represent alternate designs for Li-ion batteries.

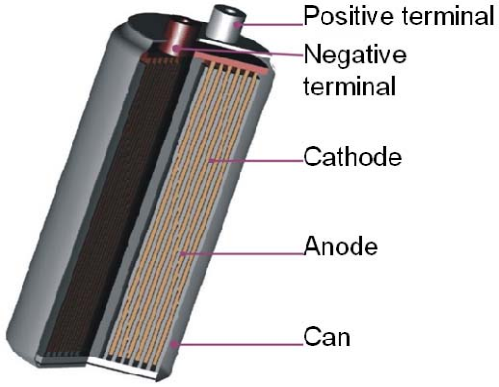

Figure 1. Schematic Showing Different Components of a Li-Ion Cell

Dissimilar material joining, hermetic sealing, localized processing, high precision, consistent quality, and high throughput are key factors for efficient battery manufacturing. Furthermore, new design concepts for compact batteries involve material combinations and joint designs that cannot be addressed using conventional thermal joining methods such as soldering, brazing, arc, and resistance spot welding. These methods have limitations regarding their speed, compatibility with other materials, and the joint designs. For example, the freedom in the joint design and the width of joint flanges strongly depend on the characteristic of the joining methods applied. The required joint accessibility, the size of the welding torch or electrodes and the heat input from the process must be taken into consideration. In addition, consistency and controllability of the welding process is important to reduce secondary operational costs.

The goal of this study was to develop laser processing technologies tailored to the specific needs in the packaging and assembly of alternative energy storage devices. Laser processing is proven in industry as a highly efficient manufacturing method with regard to productivity, enhanced performance, reliability, and lowered costs. In this investigation, the focus has been on developing manufacturing technologies to meet the demands of mass production for Li-ion batteries. The result is an array of new and highly efficient laser welding and joining technologies that will enable high volume and cost effective manufacturing.

Laser Welding of Similar and Dissimilar Materials

Most current carrying components inside a Li-ion battery are made of Cu or Al as are the external buss bars that must be joined to the outside terminals to connect a series of cells. A very reliable joining process must be applied to connect the internal parts and to seal the battery housing because of the long warranted service life (8-10 years) for HEV batteries. Joining of metals in similar and dissimilar configurations is required to establish electrical contact to the outside terminals as the connections must provide good conductivity to avoid power losses. In many cases, overlap joints are preferred since they are less demanding regarding part tolerances and fit-up.

Copper Welding

Laser welding of Cu to Cu is required in various battery joints such as connections between the negative current collector and cell terminal. Compared to steel, the welding process is more difficult to initiate on bare Cu surfaces due to its high reflectivity (~95%). Several killowatts of laser power is required to achieve sufficient intensity in the focal spot that leads to surface melting and initiate the plasma formation. The latter is required for the laser keyhole welding process with its characteristic high aspect ratio between penetration depth and weld width. Once the keyhole is established the absorption of laser radiation increases considerably and seam welding can be performed. Back reflection at process start can lead to damage of the laser resonator and beam guiding components and, therefore, must be minimized. A common industrial approach is to use a thin sheet of Ni on top of bare Cu surface or instead use Ni-plated substrates. The Ni surface absorbs the laser radiation much better and ensures a consistent start and formation of the keyhole welding process. To avoid using extra material, two alternative surface treatment methods (plasma etching/oxidation and graphite coating) were investigated to address the absorption issues.

Cu sheets were plasma etched/oxidized by heating them at very high temperatures in a oxygen-rich environment. Graphite coating was applied in form of an aerosol spray that contains highly refined graphite particles suspended in isopropyl alcohol with a special thermoplastic resin binder (Aerodag G).[(5)] A single or a multiple layer of graphite spray was applied uniformly over the sheets which resulted in thin film coating (thickness 10-20 μm) after quickly drying in the air. Both treatments resulted in more consistent welds. In comparison, the graphite coating is faster and easier to apply and provided better results. Graphite has very high electrical conductivity and is already part of the electrode material. Therefore, no immediate compatibility issues are expected from any residue that remains after welding.

Interestingly, when graphite or carbon was applied in other forms such as powered mixture, graphite chalk or black paint, it did not provide consistent results. Further improvements with regard to process stability and depth of penetration were achieved by using a small amount of oxygen as process gas.

Using optimal process parameters, two 0.5-mm-thick Cu sheets were joined (full-penetration weld) at 5.0 m/min and 2200 W laser power with graphite coating and oxygen as process gas (Figure 2). The welds were consistent and showed no defects at the surface or in the cross sections. It was also noted that the welding speed can be nearly doubled for a given penetration depth, when oxygen is supplied as a process gas at low flow rate (1 psi). No significant difference was measured in hardness across the weld nugget which proved absence of any hard oxides formed due to the use of oxygen.

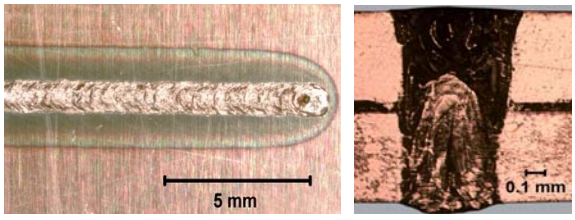

Figure 2. Top and Cross-Section View of Cu for Overlap Welding using a Multi-Mode (MM) Fiber Laser

Aluminum Welding

For cylindrical cell design, joints formed between the positive collector and the can and the sealing of the can to the lid require welding of Al. The development effort was directed towards optimization to achieve minimum porosity and weld spatter, no solidification cracking, and consistent weld quality along the complete weld length.[6] Based on input from industrial sources, Al alloys Al 1050A and Al 3003 were primarily investigated. Systematic studies showed that porosity is minimized using low line energy and helium (approximately 30 SCFH) as process gas. These conditions created a relatively small weld nugget that met the joint requirements. Using a MM fiber laser, two 1-mm-thick Al flat sheets were welded (overlap) at 1100 W and a welding speed of 3 m/min. These settings lead to a weld depth of 1.4 mm and porosity <1.4%.

Process parameters developed for flat Al sheets were transferred and further optimized for the sealing of the battery cans. A typical design of a Li-ion battery for HEVs is a cylindrical cell comprised of an Al can and lid with integrated terminals either at one or both ends. The lid must be hermetically sealed to the can. Welding trials were conducted using two different laser sources. Welds with excellent visual appearance were achieved using either a MM fiber laser at 1.9 kW and 10 m/min rotational speed or a SM (single mode) fiber laser using only 490 W of laser power at a rotational speed of 5 m/min (Figure 3). The metallographic analysis showed a good transition between the lid and the can and very low porosity without any other defects in cross section (Figure 4). The can diameter and welding speed resulted in an acceptable weld cycle time of 1.5 s per can. Compared to a MM fiber laser requiring killowatts of laser power, the results with SM fiber laser are very promising since a more cost-efficient laser source was applied.

Helium leak testing was used to determine if the joint was hermeticly sealed. The average leak rate recorded at 50 psi was 6.10^{-8}atm.cm^{3}s^{-1} which met the leak rate criteria for hermetic sealing. Test were also ran at lower pressures but no significant difference was seen in leak rates. Special lids were designed to test the burst pressure and to estimate the strength of the welds of the sealed cans. The average burst pressure was measured to be 634 psi (43.7 Bar). Moreso, the failure occurred in the can wall while the laser weld was still intact (Figure 4).

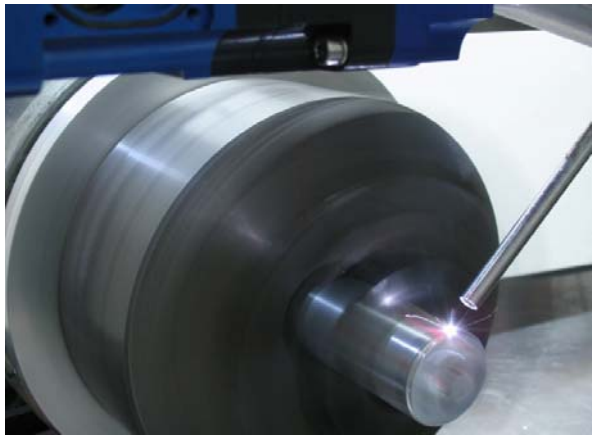

Figure 3. Laser Welding of Al Lid to Can

Figure 4. Cross Section of Welded Joint (left) - Failed Al Can after Burst Test

Stainless Steel Welding

High-speed laser welding of thin stainless steel was developed primarily applicable to the assembly of fuel cells. In a typical fuel cell, the rectangular bipolar plates are made of 0.1-mm stainless steel and have a stamped channel structure that needs to be joined to create a sealed component with internal channels. The specific tasks were (1) to apply continuous welds next to the individual channels and reinforce the structure and (2) to seal the plates along the perimeter and create a leak tight system. Different high brightness lasers (disc, MM, and SM fiber) were compared. The so-called humping effect is a limiting factor for the maximum achievable welding speed. Humping is characterized by keyhole instabilities that result in a severe undercut and the formation of periodic droplets on the weld surface.

Laser sources providing high brightness and excellent beam quality allow pushing the start of humping to much higher welding speeds. Two sheets with a thickness of 0.1 mm each were joined at a speed of 50 m/min. Figure 5 shows its surface and cross section formed with a SM fiber laser at output power of 300 W. The weld surface is very smooth and shows no signs of humping.

Figure 6 shows the maximum welding speed achieved without humping for different material thicknesses. Speeds of 70 and 40 m/min are feasible for welding two 0.05- and 0.2-mm-thick sheets in an overlap configuration.

Aluminum-Copper Welding

There are a number of battery joint designs where both excellent electrical and thermal properties of Cu and higher strength-to-weight ratio at lower price of Al would be highly desirable. Therefore, a reliable joining technique between Al and Cu and their alloys was developed.

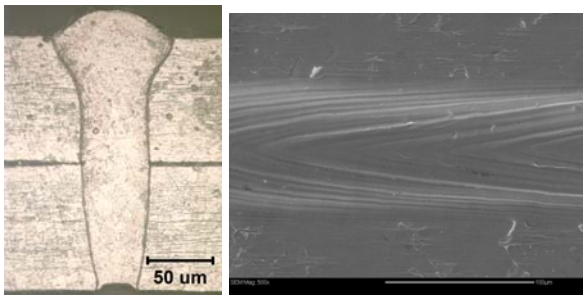

Figure 1. Overlap Penetration Weld at 50 m/min in Stainless Steel

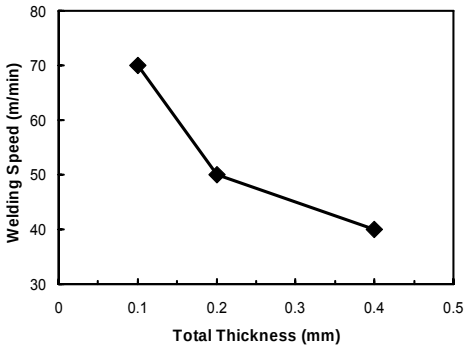

Figure 2. Maximum Welding Speed in Dependency of Material Thickness

The existing joining processes such as ultrasonic, friction, or resistance welding are often not suited for applications, which require flexible, non-contact joining techniques that only require a single side access to the joint. In contrast, the laser welding process has the potential to eliminate the majority of issues associated with dissimilar material joining. However, this requires overcoming welding challenges based on the physical and metallurgical properties of Cu-Al joints. Both metals have very low metallurgical affinity and result in the formation and growth of various intermetallic phases, which in turn can cause brittle phases, micro and macro cracks. Some approaches proposed in literature to improve the weld joint properties include (1) reducing the total number and volume of intermetallic phases in a weld microstructure, (2) eliminating the segregation of high and low melting phases, and (3) introducing a filler material, which creates favorable intermetallic phases in the welding zone.[7]

Four joint combinations were chosen based on the joint designs required for batteries. They are (1) continuous lap joining of Al on Cu, (2) continuous lap joining of Cu on Al, (3) overlap spot welding of thin Cu on Al, and (4) edge spot welding of thin Cu on Al (Figure 7). Both, pulsed and continuous wave (cw) laser sources were used to join Cu to Al.

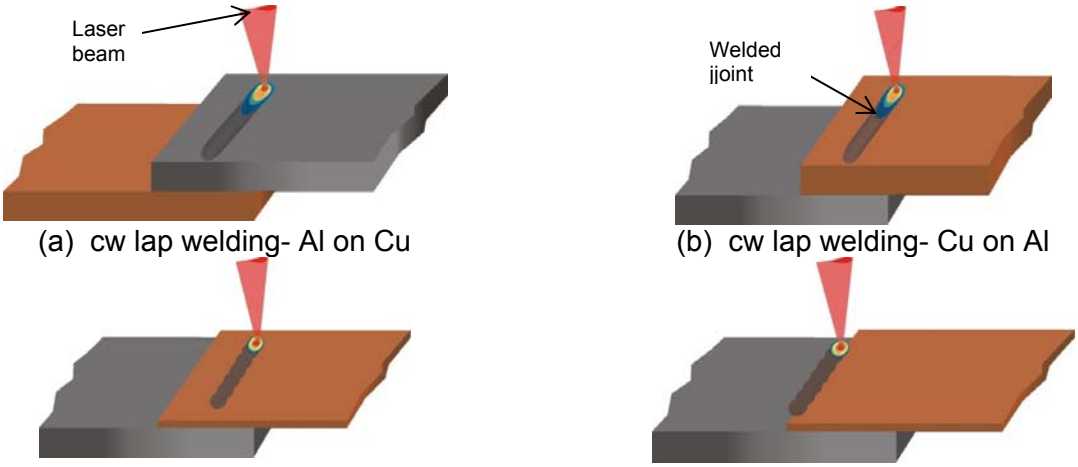

(a) cw lap welding- Al on Cu (b) cw lap welding- Cu on Al

(c) Pulsed welding- Cu on Al (d) Pulsed edge welding- Cu on Al

Figure 7. Different Joint Configurations for Welding Al to Cu

Spot welding was carried out with a pulsed Nd:YAG laser emitting at a wavelength of 1064 nm and a focusing head of 100-mm focal length. A series of optimization tests were conducted for both lap and edge welding configurations by varying pulse energy, pulse length, and focus position. Trials were also conducted by coating the top surface of Cu with graphite or using a 0.15-mm Ni foil on top of the Cu sheet to enhance the coupling and the initiation of the keyhole welding mode. Ni forms favorable alloys with Cu and Al and therefore is compatible with both materials.

Good welding results for joining 0.13-mm-thick Cu to 2.0-mm-thick Al were achieved using pulse energy of 11 J and a pulse width of 5 ms (Figure 8). The laser beam was defocused such that the focus was located 1.5 mm below the surface of the top sheet. Defocusing was used to increase the spot size and therefore the width of the weld interface. The weld penetration depth into Al was >1.0 mm. This can be a result of the high pulse energy that was required to melt through the Cu sheet into the Al.

For edge spot welding, the Cu sheet was placed on top of the Al sheet and the laser beam was aimed on the lower Al surface approximately 0.2 mm away from the edge of the Cu sheet [Figure 7(d), Figure 8]. Due to better absorption on the Al surface, it was easier to create Al melt and fuse that with the edge of the Cu sheet. It was determined that the distance between the center of the laser spot and the edge of the Cu sheet must be kept within ±0.02 mm to obtain consistent results.

Interestingly, both overlap and edge joint types showed lap shear strength of about 50-70 MPa. Higher strength of about 75-85 MPa was achieved for overlap joints, when a Ni foil was placed on top of the Cu sheet. Fatigue testing was conducted for welds that exhibited good results in lap shear testing. The samples were tested at load levels between 10 and 50% of the maximum lap shear strength and exceeded 100,000 cycles before failure.

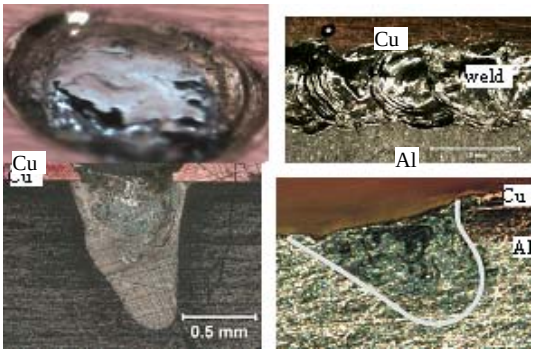

Figure 8. Top Views and Cross-Sections of Pulsed Lap (left) and Pulsed Edge (right) Welds of Cu to Al

Further, joining of Al to thicker Cu in overlap configuration was performed using a cw single-mode fiber laser (maximum power = 500 W). Welding tests were conducted between 0.55-mm-thick Al alloy 3003 and 0.6-mm-thick Cu alloy 110 at speeds between 1-2 m/min. Due to the significant difference in the melting point of both materials along with high heat conductivity, high energy input was required to melt through the top Al sheet into the Cu. As a result, the weld track was relatively wide (approximately 1.3 mm) in the Al sheet while it significantly narrowed at the interface of the Cu sheet (0.3 mm). The cross section showed that only the

high intensity peak in the center of the Gaussian laser beam penetrates approximately 0.4 mm into the Cu sheet (Figure 9). The process parameters were chosen such that only an optimal amount of Cu is mixed with the Cu-Al alloy that is formed in the weld nugget. This minimized formation and growth of intermetallic phases that could result in micro cracks. The joints showed consistent quality with some porosity but no cracks along the complete weld length.

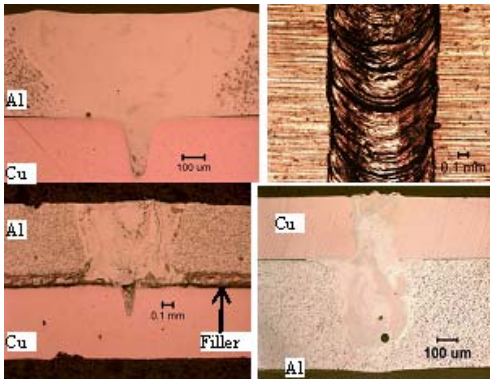

Figure 9. Top view and Cross-Sections of cw Overlap Joints of Al and Cu

Different low melting solder and filler materials (Sn, Ni and SB220-50) were applied at the interface with the intention to increase the joint strength. SB220-50® is a Sn-Ag solder alloy specifically developed for joining Cu to Al at a joining temperature of 240-260˚C. A thin film of solder material was placed between the Al and Cu sheet. During welding, the heat from the molten Al reflowed the solder alloys. While the Sn-solder and Ni did not provide any improvements in forming a stronger interface, better results were achieved with the SB220-50 solder. During welding the solder alloy reflowed next to the weld zone and connected to the Al and Cu sheet (Figure 9). The total joint interface was similar to the track width in the Al sheet. Test coupons were produced to determine the effect of the filler materials on the joint strength.

The strength and fatigue testing provided valuable data on how to further optimize the laser welding process. The lap shear load per unit length was measured for five different alloy and filler material combinations as shown in Figure 10. Based on these results, Al 3003/Cu 110 coupons welded with and without SB220-50 filler material which produced the highest lap shear load per unit length were selected for further fatigue testing.

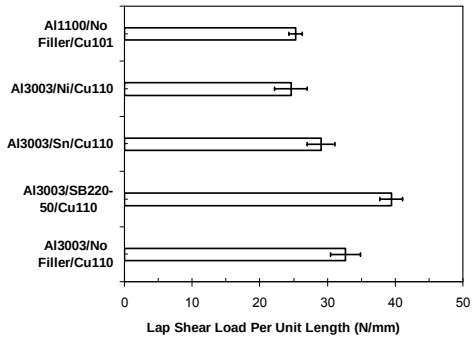

Figure 10. Maximum Lap Shear Load per Unit Length for Different Combinations of Base and Filler Material for cw Lap Joining of Al on Cu

The fatigue testing of laser joints was conducted to understand the progressive and localized structural damage that occurs when the joint is subjected to cyclic loading. The material performance under such conditions is commonly characterized by an S-N curve, also known as a Wöhler curve. The S-N curves showed clear differences between the fatigue failure properties of the two systems that were tested (Figure 11). The Al-Cu system welded without filler material had maximum shear pull strength = 652 N and sustained more than 1 million cycles for loads up to 60% of the maximum shear strength. In comparison, the joint made with filler wire had higher maximum shear strength = 788 N; however, it only passed the million cycle mark at loads up to 40% of its maximum shear strength. Tests were repeated to ascertain the higher fatigue life values for welding with/without filler and were found to be consistent within a small deviation.

SEM analysis was conducted on the failed surfaces of both Cu and Al to understand the failure pattern of these joints. Interestingly, both Cu and Al showed similar fatigue features. The width of the fatigue zone in Cu and Al was measured to be approximately ½ and ⅓ of the total bond width, respectively (Figure 12).

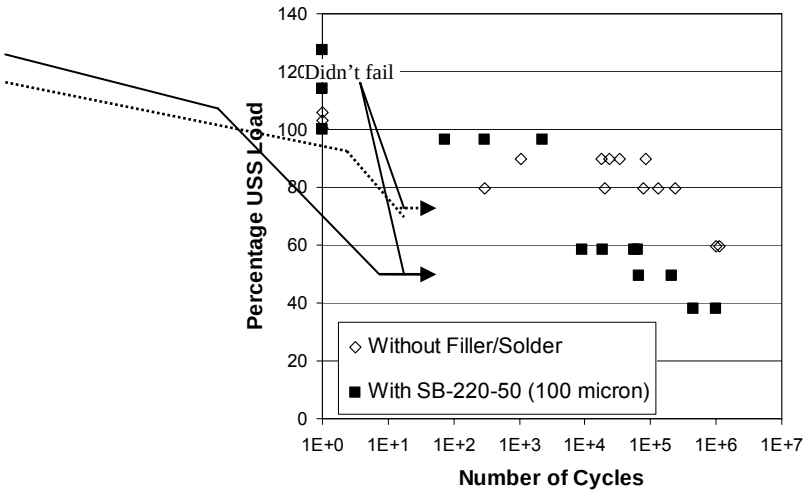

Figure 11. Fatigue Strength for cw Lap Joining of Al on Cu-Welded with and without the Filler Material

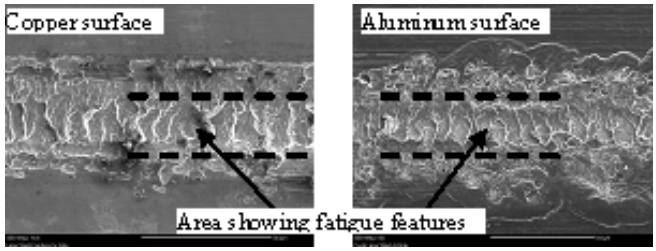

Figure 12. SEM Pictures of Fractured Weld Interfaces after Fatigue Testing on cw Lap-Joined Al to Cu

Further, TEM analysis on the fractured Cu surface showed that the fatigued zone contains approximately 92 at.% Al and 8 at.% Cu while the non-fatigued zone contains about 67 at.% Al and 33 at.% Cu (Figure 13). Based on the alloy composition in fatigued and non-fatigued zone, the following mechanism for crack propagation is proposed (Figure 14).

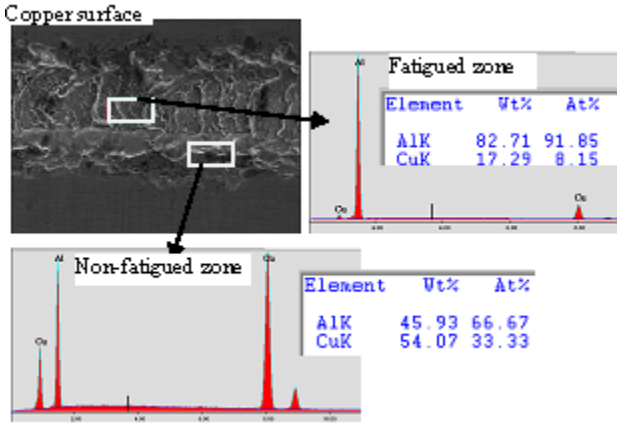

Figure 13. TEM Analysis of Fractured Weld Interfaces after Fatigue Testing on cw Lap-Joined Al on Cu

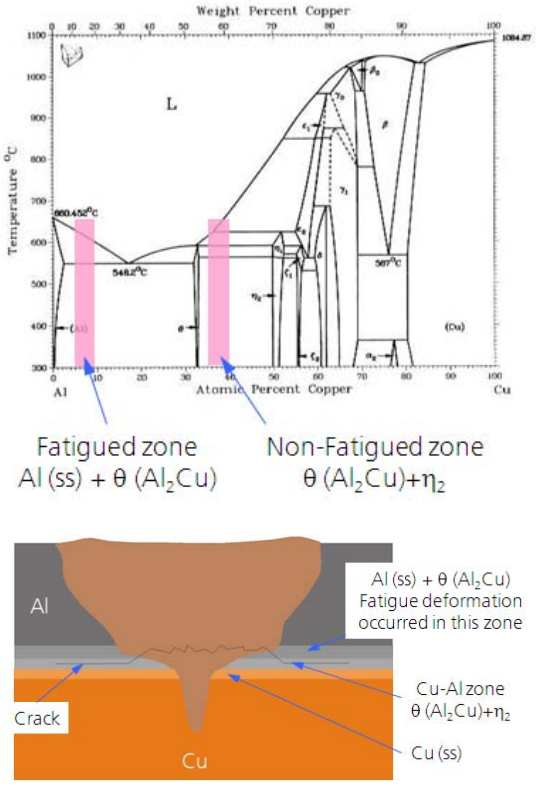

Figure 14. Cu-Al Binary Phase Diagram Showing the Phases Corresponding to Fatigued and Non-Fatigued Zones and their Respective Elemental Composition (top) - The Schematic Shows the Proposed Mechanism for Crack Propagation (bottom)

The region close to the interface can be divided in three separate layers of varying composition. The layer close to the Al is comprised of Al in solid state and θ (Al_2-Cu) phase which is rich in Al and therefore more ductile in nature. Below this layer, the composition consists of θ (Al_2-Cu) phase and η_2 phase before the composition changes into Cu in solid state in the layer. It is concluded that the cracking originates in this layer [θ (Al_2-Cu) + η_2]outside the weld width and moves to the layer above [Al solid state + θ (Al_2-Cu)]. This hypothesis is supported by TEM studies showing the phase compositions and their position in the Al-Cu binary phase diagram (Figure 14). This can explain the high fatigue strength of this joint leading to failure in the ductile, Al-rich phase.

For some joint designs, Cu needs to be placed on top of Al. Thus, welding of 0.25-mm-thick Cu alloy 110 (top) to 0.5-mm-thick Al alloy 3003 was investigated. This resulted in relatively narrow (0.2-mm) fusion zones in the Cu sheet, while the fusion zone widens significantly (0.4 mm) at the interface to the Al sheet (Figure 9). The etched cross section revealed a thorough mixing of Al and Cu phases within the fusion zone. Solidification cracking (minor and major) along the length of the weld were observed for all trials independent of the investigated parameter settings. Therefore, no strength and fatigue testing was performed for this approach.

Process Monitoring

Figure 15 shows the online monitoring system designed and built to observe the melt pool during Cu and Al welding. The laser beam has an angle of incidence of 15 degrees to the normal of the workpiece and the monitoring camera is mounted horizontally. The illumination laser beam emitted from a low-power diode laser operating at 940-nm wavelength is directed on to the workpiece using a prism placed at a 45-degree angle. The reflected laser radiation is detected by a high-speed, high-dynamic CMOS camera placed at the other end of the optical system to capture the reflected illuminated processing images of the melt pool. A frame grabber has been integrated into the proprietary software developed for coaxial process monitoring applications. This modular system can be easily modified to accommodate different input and output beam sizes, external light sources, and vision systems.

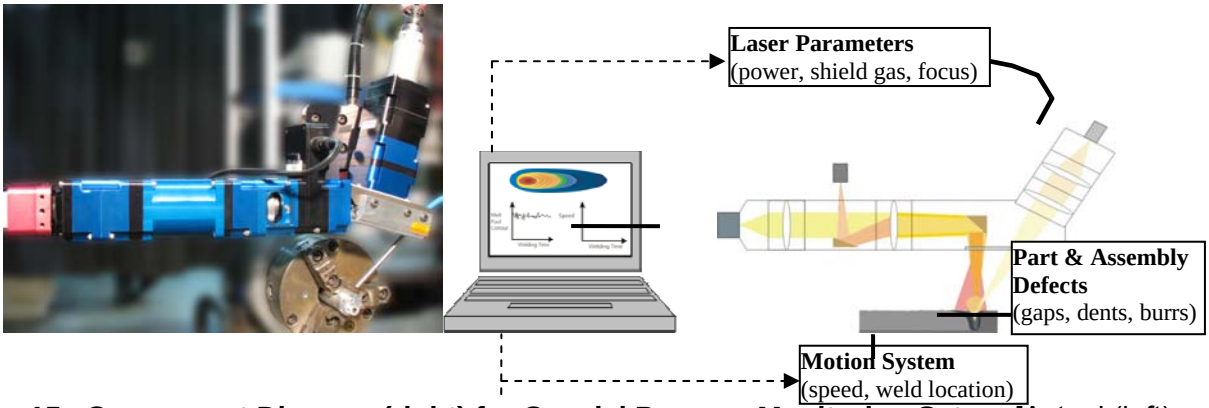

Figure 15. Component Diagram (right) for Coaxial Process Monitoring Setup [Actual (left) setup used for highly reflective metal welding.]

Due to the restricted space between processing head and workpiece, the optical system was first simulated using commercial optical design software. A component interference detection analysis was conducted to ensure that the optical path is free from any back reflection or undesired scattered radiation. In addition, the software was updated for more efficient data collection tailored to the modified optical setup. Figure 15 exhibits the information flow for the

overall process. It shows the different possible changes in the process conditions related to laser system, motion system, or part quality that can directly influence the weld outcome and therefore need to be monitored. The goal was to first simulate these changes on simpler geometries such as the flat coupons and then transfer the know-how to actual battery parts production.

Initially, the process for overlap welding of flat Al-alloy sheets was monitored. Figure 16 shows the difference in images obtained with and without illumination. Without additional illumination, only a small amount of plasma radiated from the welding process is detected and provides limited information about the location of the melt pool (glowing red spot). With proper illumination, meltpool, keyhole, and weld are clearly visible. Using this image, the size (length and width) and location of the melt pool can be measured in real-time and any deviation can be used for detecting process deviations from the optimum settings.

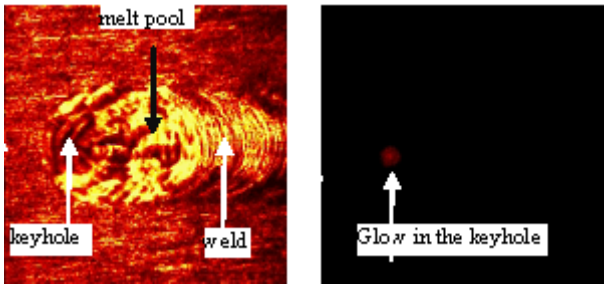

Figure 16. High-Speed Camera Pictures of Welding Process Showing the Melt Pool with (left) and without (right) Coaxial Illumination.

The process monitoring system was validated for sealing of battery cans. A comprehensive study was carried out where different types of process and part defects were simulated, typically found in industrial setups. Table 1 shows the investigated types and causes of defects and their effect on the monitored condition (melt pool size). It can be seen that the changing pattern in melt pool width and length is different for each defect. This allowed to relate a specific defect to a particular pattern of signal and therefore provided information to distinguish between various defects occurring simultaneously. Since the sealing of battery cans need to meet stringent requirements regarding hermeticity and weld strength, the real-time process monitoring system offers a quality check on 100% of the products without interrupting the production cycle.

Summary and Conclusions

The laser processing capabilities applicable to the assembly and packaging of batteries and fuel cells has been discussed. Laser welding of similar and dissimilar material combinations showed the application domain and advantages of using this technology.[8]

Fast and robust laser welding processes were developed for Cu-to-Cu, stainless steel-to-stainless steel and Al-to-Al (similar material combinations). Sealing of Al cans was performed using a relatively low-power and low-cost laser source at speed up to 5 m/min. Further testing on sealed cans showed that the hermetic sealing was achieved and very high burst pressure was recorded. Thin stainless steel was welded at speeds >50 m/min without humping effect commonly associated at these high speeds.

Table 1. Effect of Irregularities in Welding of Battery Cans on Melt Pool Width and Length

SN	Type of Defect	Cause of Defect	Effect of Defect on Monitored Condition	
1	Insufficient penetration depth	Laser system (power, speed, focus position)	Both meltpool width and height changes gradually	
2	Misalignment with weld seam	System setup, parts issue	Ratio of meltpool width to height fluctuates	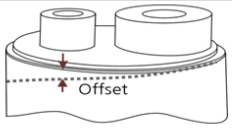
3	Low/No Gas pressure	System setup	Both meltpool width and height fluctuates highly	
4	Too large gap at weld seam	Parts issue, assembly issue	Meltpool height fluctuates highly	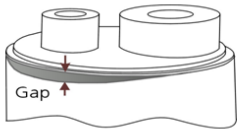
5	Defective parts such as dents, burrs etc.	Parts issue	Both meltpool width and height varies randomly	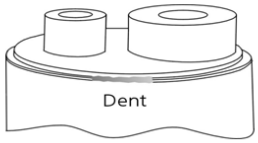

Welding of dissimilar material was mainly focused on joining Al and Cu in a variety of configurations using both pulsed and continuous welding techniques. Excellent welding quality was achieved with process optimization based on thorough characterization of welded areas followed by mechanical testing. Strength measurements clearly showed the improvement achieved by using different filler materials and joining conditions. Furthermore, fatigue results proved the durability of Cu-to-Al welds. Test coupons survived more than 1 million fatigue cycles at 60% USS.

Online process monitoring results were presented for welding flat sheet combinations of highly reflective materials (Cu and Al) and were later applied for sealing of battery cans. Most of the common defects encountered in production of such parts were identified correctly for both flat samples and actual battery parts. The variation of meltpool length and width was shown to be directly affected by these defects. Similar correlation could be developed for other joint designs and material combinations.

In conclusion, an array of new, reliable, and very efficient laser manufacturing processes suited for the production of advanced batteries and other applications in the field of alternative energy devices has been developed along with integrated quality control techniques.

Acknowledgements

This work is supported by a grant from the State of Michigan's 21st Century Jobs Fund, which we gratefully acknowledge.

References

(1) International Conference on Advanced Lithium Batteries for Automobile Applications, Argonne, IL (Sept. 15-17, 2008).
(2) Boston Consulting Group, "The Comeback of the Electric Car? How Real, How Soon, and What Must Happen Next" (Jan. 2009).
(3) Muller, J. and Stone, A., “Jump Start”, *Forbes* (Apr. 2008).
(4) McDowall, J., “Understanding Lithium-Ion Technology”, *Battcon*, Marco Island, FL (Apr. 2008).
(5) www.achesonindustries.com.
(6) Herfurth, H. J., Patwa, R., Pantsar, H., Heinemann, S., and Newaz, G., “Laser Processing for Alternative Energy Devices: Advanced Battery and Fuel Cell Applications”, *ICALEO*, Temecula, CA (Oct. 2008).
(7) Mys, I. and Schmidt, M., “Laser Micro Welding of Copper and Aluminum”, *Proc. of SPIE*, Vol. 6107, 610703 (2006).
(8) Herfurth, H. J, “Building Better Batteries”, *Industrial Laser Solutions* (May 2009).